

Comparison of higher-order mode suppression and Q-switched laser performance in thulium-doped large mode area and photonic crystal fibers

Pankaj Kadwani,* Clemence Jollivet, R. Andrew Sims, Axel Schülzgen, Lawrence Shah, and Martin Richardson

CREOL, The College of Optics and Photonics, Building 53, 4000 Central Florida Blvd., Orlando, FL 32816, USA
*pkadwani@creol.ucf.edu

Abstract: We report the influence of higher order modes (HOMs) in large mode fibers operation in Q-switched oscillator configurations at ~ 2 μm wavelength. S^2 measurements confirm guiding of LP_{11} and LP_{02} fiber modes in a large mode area (LMA) step-index fiber, whereas a prototype photonic crystal fiber (PCF) provides nearly single-mode performance with a small portion of light in the LP_{11} mode. The difference in HOM content leads to a significant difference in Q-switched oscillator performance. In the step-index fiber, the percentage of cladding light increases by 20% to $>40\%$ with increasing pulse energy to ~ 250 μJ . We attribute this degradation to saturation of the gain in the fundamental mode leading to more light generated in the HOMs, which is eventually converted into cladding light. No such degradation is seen in PCF laser system for >400 μJ energies.

©2012 Optical Society of America

OCIS codes: (060.3510) Lasers, fiber; (140.3540) Lasers, Q-switched; (060.2420) Fibers, polarization-maintaining; (060.5295) Photonic crystal fibers.

References and links

1. <http://www.advaluephotonics.com/2-micron-fiber-laser-products.html>
2. <http://www.npphotonics.com/>
3. http://www.nufern.com/pam/fiber_lasers/family/id/11/recnum/0/
4. http://www.ipgphotonics.com/products_2micron_laser_cw.html
5. G. D. Goodno, L. D. Book, and J. E. Rothenberg, "600 W Single-mode, single-frequency Thulium fiber laser amplifier," *Proc. SPIE* **7195**, 71950Y, 71950Y-10 (2009).
6. G. Imeshev and M. E. Fermann, "230-kW peak power femtosecond pulses from a high power tunable source based on amplification in Tm-doped fiber," *Opt. Express* **13**(19), 7424–7431 (2005).
7. L. Dong, T. Wu, H. A. McKay, L. Fu, J. Li, and H. G. Winful, "All-glass large-core leakage channel fibers," *IEEE J. Sel. Top. Quantum Electron.* **15**(1), 47–53 (2009).
8. C. Liu, G. Chang, N. Litchinitser, A. Galvanauskas, D. Guertin, N. Jacobson, and K. Tankala, "Effectively single-mode chirally-coupled-core fiber," in *OSA/ASSP. ME2* (2007).
9. J. C. Knight, T. A. Birks, P. St. J. Russell, and D. M. Atkin, "All-silica single-mode optical fiber with photonic crystal cladding," *Opt. Lett.* **21**(19), 1547–1549 (1996).
10. C. D. Brook and F. Di Teodoro, "Multimegawatt peak-power, single-transverse-mode operation of a 100 μm core diameter, Yb-doped rodlike photonic crystal fiber amplifier," *Appl. Phys. Lett.* **89**(11), 111119 (2006).
11. T. Eidam, J. Rothhardt, F. Stutzki, F. Jansen, S. Hädrich, H. Carstens, J. Limpert, and A. Tünnermann, "Fiber CPA system delivering 2.2 mJ, sub 500 fs pulses with 3.8 GW peak power," in *OSA/ASSP ATuD3* (2011).
12. F. Stutzki, F. Jansen, A. Liem, C. Jauregui, J. Limpert, and A. Tünnermann, "26 mJ, 130 W Q-switched fiber-laser system with near-diffraction-limited beam quality," *Opt. Lett.* **37**(6), 1073–1075 (2012).
13. <http://www.nktp Photonics.com/files/files/DC-200-40-PZ-Yb-03-110817.pdf>
14. http://www.nufern.com/pam/optical_fibers/searchresult/id_category/3/recnum/0/
15. K. Tankala, B. Samson, A. Carter, J. Farroni, D. Machewirth, N. Jacobson, U. Manyam, A. Sanchez, M. Y. Chen, A. Galvanauskas, W. Torruellas, and Y. Chen, "New developments in high power eye-safe LMA fibers," *Proc. SPIE* **6102**, 610206, 610206-9 (2006).
16. N. Modsching, P. Kadwani, R. A. Sims, L. Leick, J. Broeng, L. Shah, and M. Richardson, "Lasing in thulium-doped polarizing photonic crystal fiber," *Opt. Lett.* **36**(19), 3873–3875 (2011).
17. P. Kadwani, N. Modsching, R. A. Sims, L. Leick, J. Broeng, L. Shah, and M. Richardson, "Q-switched thulium-doped photonic crystal fiber laser," *Opt. Lett.* **37**(10), 1664–1666 (2012).

18. J. W. Nicholson, A. D. Yablon, S. Ramachandran, and S. Ghalmi, "Spatially and spectrally resolved imaging of modal content in large-mode-area fibers," *Opt. Express* **16**(10), 7233–7243 (2008).
19. M. Eichhorn and S. D. Jackson, "High-pulse-energy actively Q-switched Tm³⁺-doped silica 2 microm fiber laser pumped at 792 nm," *Opt. Lett.* **32**(19), 2780–2782 (2007).
20. S. D. Jackson and S. Mossman, "Efficiency dependence on the Tm³⁺ and Al³⁺ concentrations for Tm³⁺-doped silica double-clad fiber lasers," *Appl. Opt.* **42**(15), 2702–2707 (2003).
21. G. P. Frith and D. G. Lancaster, "Power scalable and efficient 790-nm pumped Tm³⁺-doped fiber lasers," *Proc. SPIE* **6102**, 610208, 610208-10 (2006).
22. G. Turri, V. Sudesh, M. Richardson, M. Bass, A. Toncelli, and M. Tonelli, "Temperature-dependent spectroscopic properties of Tm³⁺ in germanate, silica, and phosphate glasses: A comparative study," *J. Appl. Phys.* **103**(9), 093104 (2008).
23. D. L. Sipes, J. D. Tafoya, D. S. Schultz, B. G. Ward, and C. G. Carlson, "Advanced components for multi-kW fiber amplifiers," *Proc. SPIE* **8237**, 82370P, 82370P-6 (2012).
24. D. Creeden, P. A. Budni, P. A. Ketteridge, T. M. Pollak, E. P. Chicklis, G. Frith, and B. Samson, "High power pulse amplification in Tm-doped fiber," in *OSA/CLEO/QELS* (2008)
25. Y. Tang, L. Xu, Y. Yang, and J. Xu, "High-power gain-switched Tm³⁺-doped fiber laser," *Opt. Express* **18**(22), 22964–22972 (2010).
26. L. Shah, R. A. Sims, P. Kadwani, C. C. C. Willis, J. B. Bradford, A. Pung, M. Poutous, E. G. Johnson, and M. Richardson, "Integrated Tm: fiber MOPA with polarized output and narrow linewidth with 100 W average power," *Opt. Express* **20**(18), 20558 (2012).

1. Introduction

Thulium based fiber technology has matured in the last decade and is now the basis for a wide range of commercial systems providing amplified spontaneous emission (ASE), as well as CW and pulsed laser sources [1–4]. In the development of high peak-power fiber lasers, the primary limitations on scalability are associated with nonlinear phenomenon such as stimulated Brillouin scattering (SBS), stimulated Raman scattering (SRS), and self-phase modulation (SPM). Relative to Yb- and Er-doped fiber lasers, the longer wavelength of Tm offers the significant potential benefit of lower nonlinearity since SBS, SRS, and SPM thresholds scale proportionately with wavelength. To date, several notable laser performance results have been achieved using conventional step-index Tm-doped fibers operating in the 2 μ m wavelength regime. For example, Goodno et al. demonstrated CW single-frequency output with 600 W [5] with $M^2 \sim 1.05$ and Imeshev et al. achieved 230 kW peak power in the fiber while amplifying ultrashort laser pulses [6].

Regardless of operational wavelength, large mode area (LMA) fiber designs are required to suppress nonlinearities in order to generate and guide pulses with high peak power. In most application areas for such high peak power pulses, quasi diffraction-limited beam quality is also critical. Thus, the fundamental challenge is to achieve the largest possible mode area while still maintaining high beam quality. In step-index fibers, the mode area is inversely proportional to the numerical aperture (NA) between the core and cladding as defined by the V parameter. Unfortunately, for practically achievable NAs, LMA step-index fibers typically guide several transverse modes.

In order to increase single-mode area beyond what is possible with conventional step-index fibers, several alternative fiber designs have been developed for Yb-doped fibers. Leakage channel fibers (LCF) are designed such that all modes, including the fundamental, experience waveguide losses; however the loss for the fundamental mode is orders of magnitude less than for higher order modes making it possible to achieve nearly single-mode output with ultra-large mode area [7]. Chirally coupled core (CCC) fibers achieve ultra-large mode area via a secondary waveguide, which is wrapped helically around the central core to cause higher propagation loss for higher order modes than the fundamental mode [8].

However, the most extensively investigated design for achieving ultra large mode area with quasi single-mode beam quality is photonic crystal fiber (PCF) [9]. A 100 μ m core rod type PCF has been used to generate 4.3 MW peak power ns pulses with single mode and linearly polarized output [10]. To date, the highest extracted peak power from any fiber laser system is 3.8 GW with 480 fs pulses in 108 μ m core PCF [11]. Scaling up the core diameter further to 135 μ m has enabled the generation of 26 mJ, sub 60 ns pulses [12]. Only recently

has PCF technology been applied to thulium doped fiber lasers operating at $\sim 2 \mu\text{m}$ wavelength.

Figure 1(a) shows the end facet image of a Tm-doped PCF (fabricated by NKT Photonics A/S), which consists of a hexagonal air lattice surrounding the core. The micro-structured cladding makes it possible to achieve much smaller effective NA (< 0.03) than conventional LMA step-index fiber (0.06) in a standard Yb-doped configuration [13,14]. We compare this novel PCF fiber with a state-of-the-art Tm-doped step-index LMA fiber (fabricated by Nufern) with a cross section as shown in Fig. 1(b). The core is co-doped with aluminum in order to improve efficiency and avoid photodarkening, which increases the index of refraction of the core well above that of the cladding [15]. In order to reduce the NA of the core, a refractive index pedestal is incorporated into the cladding. In this fiber, the result is an effective core NA of 0.09 as compared to the ~ 0.15 NA of the core glass to the cladding without the refractive index pedestal. Unfortunately, it is not currently feasible to reduce to core NA below 0.09 in this silica fiber even with the pedestal, thus the step-index LMA fiber guides multiple transverse modes.

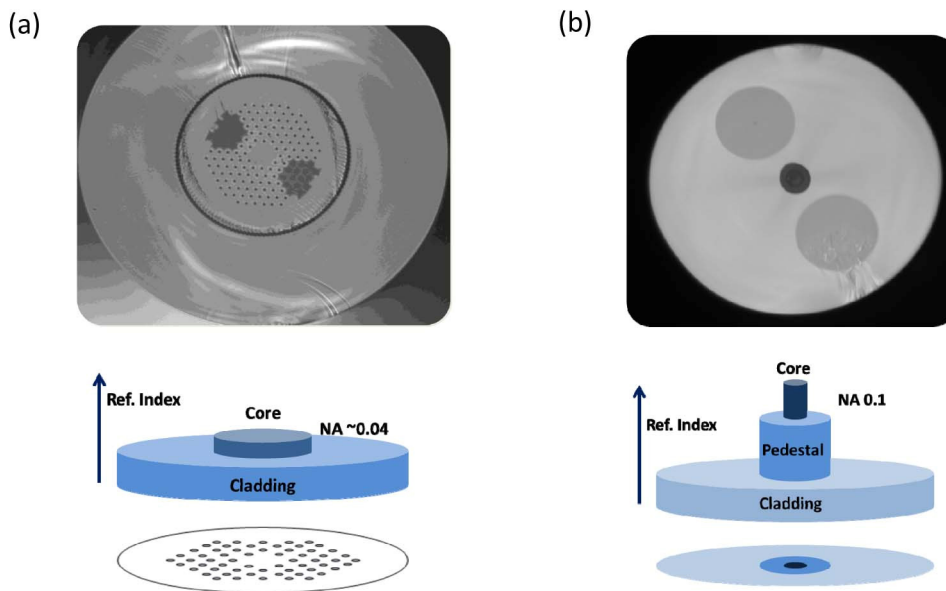


Fig. 1. a) The end facet and typical refractive index profile for the Tm-doped photonic crystal fiber (not to scale) with an effective NA of ~ 0.04 . b) The end facet and refractive index profile for a Tm-doped LMA fiber with a refractive index and 0.1 core NA.

To the best of our knowledge, besides step-index LMA, the PCF concept is the only LMA fiber architecture that has been adapted for use with Tm doping. We have recently reported the cw performance of a PCF with 50 μm core diameter and $\sim 36 \mu\text{m}$ mode field diameter (MFD), experimentally generating highly polarized light at 2 μm with $M^2 < 1.15$ [16]. We have also shown that this fiber is well suited for the generation of nanosecond laser pulses, producing 435 μJ energy pulses with 49 ns pulse duration in a Q-switched oscillator cavity [17]. For the first time, we investigate and compare the modal properties of PCF and step-index LMA fibers in the 2- μm wavelength regime and utilize these results to explain the Q-switched oscillator performance of thulium doped fiber lasers.

2. Modal characteristics from S^2 measurements

M^2 is a common parameter to quantify laser beam quality, but has limited utility when a relatively small portion of power is carried by higher order modes (HOMs). In such cases the shape of the beam remains Gaussian-like $M^2 \sim 1$. When operating at high power, even very

low HOM content can cause significant beam distortions and pointing instabilities emphasizing the need for high-resolution modal composition analysis.

Spatially and spectrally resolved imaging (S^2 imaging) is a recently demonstrated technique, which can identify the transverse modes of an LMA fiber and the power distribution among the modes down to -30 dB from the peak [18]. In the presented work, for the first time to our knowledge, we apply the same technique to characterize the modal content guided in the $2\ \mu\text{m}$ wavelength regime for step-index and PCF large mode area (LMA) fiber designs. The output signal from an ASE source based upon single-mode Tm:fiber with $10\ \mu\text{m}$ core diameter and $130\ \mu\text{m}$ cladding diameter is coupled into the core of the fiber under test. This source produces a broadband spectrum from $1980 - 2020\ \text{nm}$, and the transmitted signal is recorded using an optical spectrum analyzer (OSA) $1200 - 2400\ \text{nm}$ from Yokogawa. The spectra are recorded by scanning a butt-coupled single-mode fiber spatially across the output facet of the LMA under test, providing spatially resolved measurement of any multi-mode interference (MMI). Data recording and spatial scanning are automated using a Labview interface. The Fourier transform (FT) of each spectrum provides a measure of the relative group delay between the fundamental mode and any guided HOM at a specific spatial location. Finally, all the FT spectra are combined from which the two dimensional profile and power distribution across all the modes propagating in the fiber core are extracted for powers levels as low as $30\ \text{dB}$ below the peak [18].

We performed S^2 measurements on passive samples of PCF and LMA fibers where the structure dimensions are matched as closely as possible to the Tm-doped versions used in the Q-switched laser systems. Due to ground state absorption (albeit weak) from the three-level laser nature of thulium, it was not possible to perform S^2 imaging of thulium-doped fiber samples using our ASE source centered at $2\ \mu\text{m}$. As such, we have not yet been able to investigate any differences in refractive index profile between passive and active fibers. However, this modal investigation of passive samples is the first rigorous characterization multimode or quasi-single mode character of the fibers in the $2\ \mu\text{m}$ wavelength regime. By characterizing the HOM content as a function of the coiling diameter, we are able to determine the relative bend losses for the guided modes.

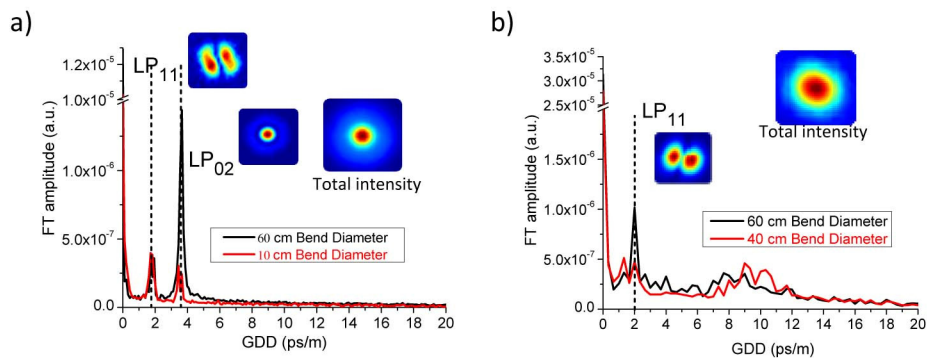


Fig. 2. S^2 data revealing guided mode content around wavelengths of $2\ \mu\text{m}$: a) PM-LMA fiber, and b) PCF.

One sample is a $3.1\ \text{m}$ long double-clad step-index polarization maintaining (PM) LMA fiber with $25\ \mu\text{m}$ diameter, 0.09 NA core and $400\ \mu\text{m}$ outer diameter, 0.22 NA cladding. The second sample is a $1.6\ \text{m}$ long prototype polarizing double-clad PCF with a $50\ \mu\text{m}$ core diameter, 0.04 NA and $250\ \mu\text{m}$ cladding diameter, and 0.45 NA. The mode content of each fiber is measured for different coiling diameters with optimized coupling of the single mode ASE source. For symmetric facet coupling of the ASE signal and relatively large coiling diameter (60cm) to minimize bend-induced HOM suppression, the LMA fiber supports LP_{01} , LP_{11} , and LP_{02} modes (Fig. 2(a)) and the PCF sample supports LP_{01} and LP_{11} modes (Fig.

2(b)). We plot the modal content for large coiling diameter along with the minimum-coiling diameter possible before inducing significant loss for the fundamental mode in both fibers. The beam intensity profile as well as the mode profiles are reconstructed from the FT at the group delay difference (GDD) characteristic of the interference between the HOM and the fundamental mode. Under symmetric excitation with 60 cm coil diameter, up to 40% of the total power coupled in the LMA fiber is guided via the LP_{02} mode and 4% in LP_{11} . As expected, under axial excitation, the power is mainly coupled into centro-symmetric modes of the form LP_{0n} (56% in LP_{01} and 40% in LP_{02}) while significantly less power is coupled into LP_{11} . Coiling the LMA sample to 10 cm diameter induces 10 dB loss in LP_{02} and less than 1 dB loss in LP_{11} ; however $\sim 5\%$ of the power remains in HOMs. By comparison, the PCF is much closer to single mode even for large coiling diameter; only 4.3% of the total power is guided in the LP_{11} mode and LP_{02} is not supported, as shown on Fig. 2(b). Additional coiling to 40 cm diameter reduces the modal content in LP_{11} to $<1\%$ power levels enabling quasi-single mode operation.

3. Effect of modal properties on laser performance

In order to examine the impact of the modal properties of these fibers on the laser performance, we compare Tm-doped versions of both fibers as the gain medium in Q-switched laser oscillators. The system schematic (Fig. 3(b)) is similar to that used by Eichhorn and Jackson [19] with the primary differences being that the fibers under test are PM and that the cavity is single-end pumped in a co-propagating configuration.

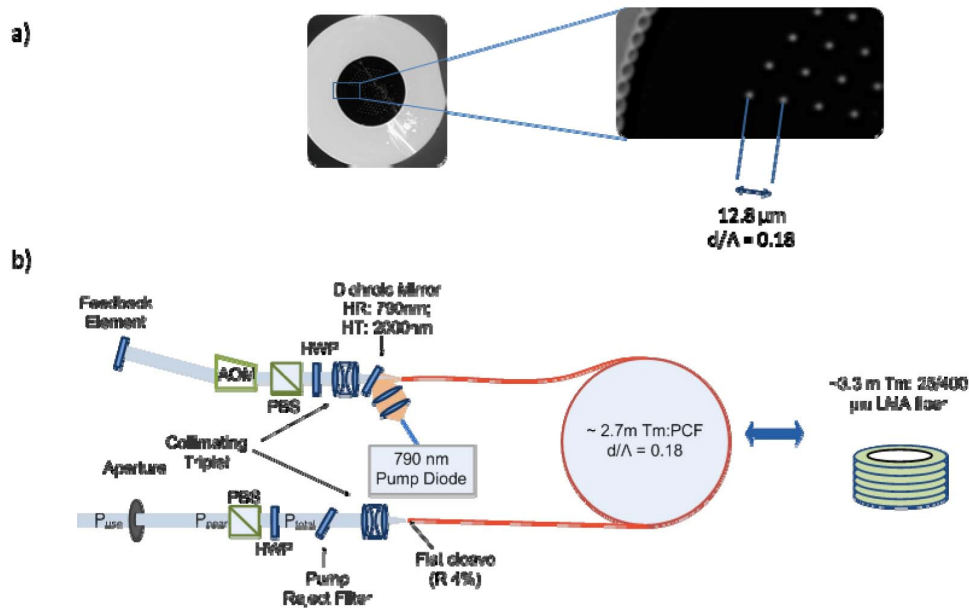


Fig. 3. a) The Tm:PCF with diameter to pitch ratio of 0.18 was used for the experiments. b) Q-switched laser oscillator schematic. The two fiber types Tm: PCF and Tm: LMA were exchanged while keeping all other components the same for comparative testing. (AOM: Acousto-optic modulator, HWP: Half wave plate, PBS: Polarizing beam splitter).

The pump is a 100 W, 793 nm diode laser (DILAS Diode Laser, Inc.) with 200 μm diameter core, 0.22 NA delivery fiber. The pump is coupled into the fiber using a 1:1 telescope (consisting of two 25 mm diameter, 50 mm focal length achromatic doublet lenses) and the reflection from a dichroic mirror (HR 790 nm, HT 2000 nm). In the free-space Q-switch portion of the cavity, the fiber output is collimated using a 26 mm focal length Infrasil triplet lens and propagates through a polarizing beam splitter and half-waveplate to an acousto-optic modulator (AOM), which deflects $\sim 66\%$ of the beam into the 1st diffraction

order. The diffracted beam is fed back into the cavity with a highly reflective mirror, whereas the 0th order beam is blocked to prevent free lasing. For each fiber, the intracavity fiber facet is angle cleaved to prevent parasitic lasing and the output fiber facet is flat cleaved to serve as the output coupler. The output of the oscillator is collimated with a 26 mm Infrasil triplet lens and a dichroic pump rejection filter eliminates the residual pump light. The total output power, P_{total} , is measured immediately after the collimator and pump rejection filter. A half wave plate (HWP) and PBS transmit only the portion of the oscillator output that is p-polarized. An aperture is used to block any signal light guided outside the signal core; thus, the usable output power corresponds to P_{use} .

Using the same cavity setup, we compare the Q-switched laser performance of two Tm-doped LMA fibers: a step-index fiber double clad and polarization maintaining (PM) with core/cladding diameters of 25/400 μm and 0.09 NA (PLMA-TDF-25P/400-HE manufactured by Nufern), and a PCF double clad and polarizing fiber with core/cladding diameters of 50/250 μm and 0.04 NA (DC-250/50-PM-Tm manufactured by NKT Photonics A/S). The step-index LMA fiber core is doped with 4 wt.% Tm_2O_3 , and the ~ 3.3 m long active fiber (~ 2.4 dB/m absorption at 793 nm) is spliced to passive LMA leads, making the total fiber length ~ 4.5 m. The active PCF is doped with 2.5 wt.% Tm_2O_3 , is ~ 2.7 m long (~ 5.8 dB/m absorption at 793 nm) and has hexagonal lattice of air-holes with hole-size to pitch (d/Λ) ratio of 0.18 with a pitch of 12.8 μm (Fig. 3(a)). The pump is guided within the 250- μm diameter air cladding (Fig. 1(a)) with 0.45 NA. Boron doped stress rods are incorporated into the air hole lattice producing a birefringence $> 1 \times 10^{-4}$. The PCF end faces were prepared by first collapsing the holes using a Vytran GPX-3400 splicer and then cleaving them using a LDC-200 cleaver.

As mentioned above, passive fiber sections were spliced to the active step-index fiber. Thus, the entire length of active step-index fiber could be wrapped around an 11.5 cm diameter mandrel water-cooled to $\sim 13^\circ\text{C}$. Unlike the step-index fiber, it was not possible to efficiently cool the entire length of the PCF due to its relatively large 35 cm operational bend diameter and the fact that it was not feasible to splice to passive fiber sections. In these experiments, the pump light was coupled into a ~ 28 cm long portion of the PCF mounted in a straight water-cooled V-groove at $\sim 13^\circ\text{C}$ whereas the remaining length was air-cooled.

4. Differences between LMA and PCF laser performance

To accurately determine the percentage of the total output power/energy that would be available for an application such as pumping a mid-IR optical parametric amplifier, we compare P_{total} and P_{use} as shown in Fig. 3. Figures 4(a) and 4(b) show the slope efficiency for P_{total} relative to the launched power for the step-index fiber and PCF respectively. In both 4(a) and 4(b), the slope efficiency increases by $\sim 6\%$ when the repetition rate is increased from 10 to 20 kHz, with a maximum slope efficiency of 36.3% for step-index fiber and 31.8% for PCF at 20 kHz. This difference in performance cannot be explained in terms of the lengths of the active fibers and their respective pump absorption, as the PCF has significantly higher absorption than the step-index fiber.

For the PCF (Fig. 4(d)), the slope efficiency reduces to 25.8% at 20 kHz and 20.2% at 10 kHz when P_{use} is plotted vs. launched pump. However in the case of the step-index, fiber the slope significantly deviates from a linear fit, particularly at 10 kHz repetition rate. The maximum amount of usable power is about 80% of the total for the PCF and step-index fiber at low power. This includes the reflection losses of the PBS and the waveplate ($\sim 6\%$), light in the rejected polarization, and any signal light trapped in the cladding. In low power cw tests, the step-index fiber displayed $\sim 11\%$ cladding light whereas the PCF showed $\sim 14\%$ cladding light at ~ 44 cm bend diameter.

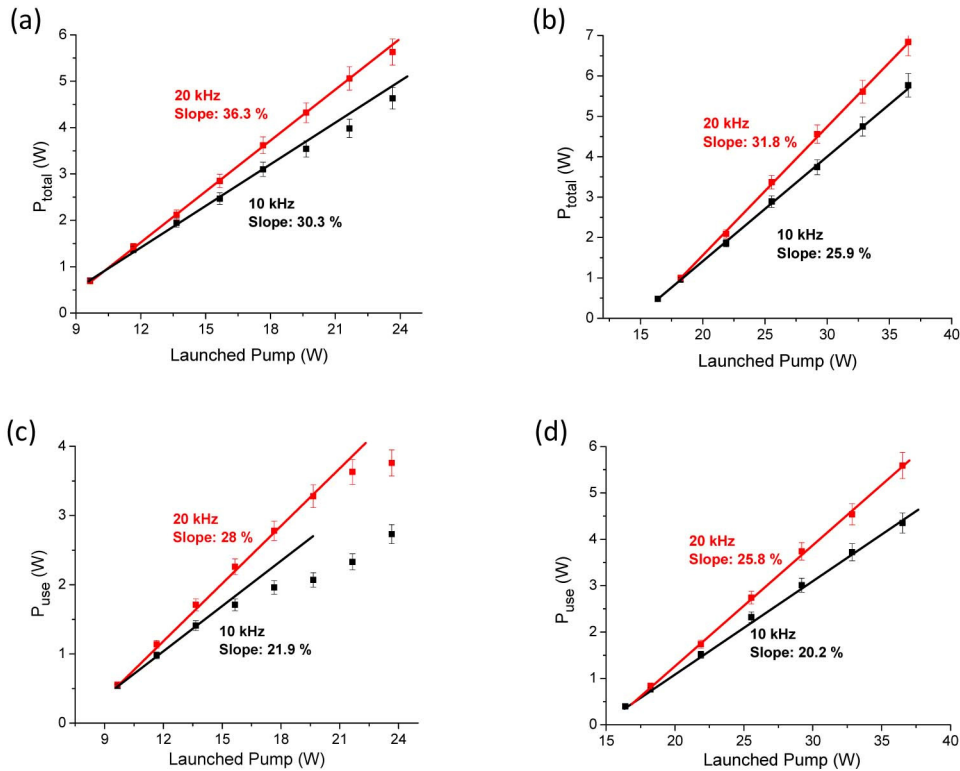


Fig. 4. The top two plots show the total average output power slope efficiency for a) LMA fiber oscillator and b) PCF oscillator. These are compared to the usable polarized output power c) LMA fiber oscillator and d) PCF oscillator. All the above measurements are shown for 10 and 20 kHz repetition rate.

The PCF in general showed lower slope efficiencies as compared to the step-index fiber. We believe this is primarily due to the different glass compositions in the two fibers. The significance of Tm^{3+} concentration and Al^{3+}/Tm^{3+} concentration ratio on the slope efficiency in 790 nm pumped Tm:silica fiber lasers has been outlined by S.D. Jackson in [20]. In addition to the lower Tm^{3+} concentration in PCF, the Al^{3+}/Tm^{3+} ratio is also lower in PCF (8:1) as compared to the ~10:1 ratio in step-index fibers [21].

The difference between the modal performance of the step-index fiber and the PCF becomes evident when the percentage of usable output is plotted as a function of total output pulse energy (Fig. 5). As such, it is clear that the percentage of usable output degrades significantly for the step-index fiber as a function of pulse energy (Fig. 5(a)) and reaches a minimum of ~58% for energies >200 J. On the other hand, the usable output percentage for the PCF remains constant for almost all pulse energies with a slight decrease to ~75% at 435 J at 10 kHz. We believe that this degradation in usable output is not thermal in nature, as it is linked to the pulse energy in the step-index fiber independent of the pulse repetition rate.

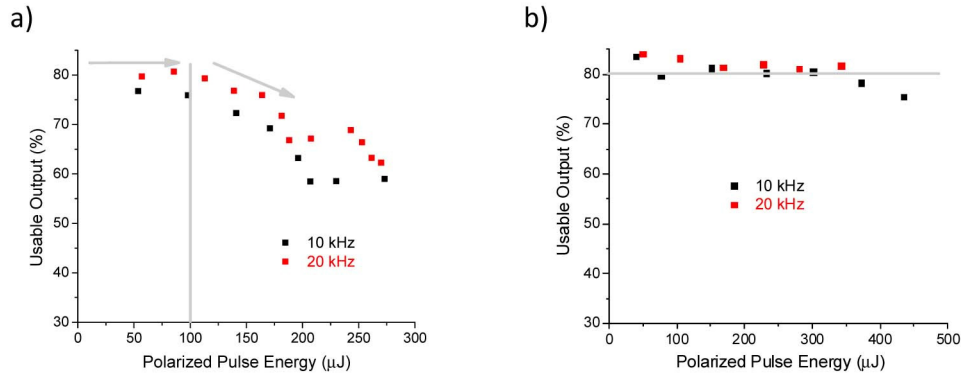


Fig. 5. The usable output in the core as a percentage of total power (core + cladding) with respect to pulse energy obtained for a) LMA fiber and b) PCF at 10, 20 and 50 kHz repetition rates.

Figure 6 shows the pulse-width for the step-index and PCF oscillators as a function of launched pump. For the step-index (Fig. 6(a)), the minimum pulse duration is 150 ns pulse duration for both 10 and 20 kHz repetition rate, whereas the minimum pulse duration is 49 ns for the PCF at 10 kHz (Fig. 6(b)). The difference in minimum pulse duration can be partially attributed to the difference in total fiber length, such that the cavity round trip time is ~ 49 ns for the step-index fiber case vs. ~ 31 ns for the PCF. However, comparing Fig. 6(a) and 4(c) shows that the pulse duration in the step-index fiber approaches the minimum value at roughly the same pump power at which the slope efficiency starts diverging from linear i.e. ~ 16 W for 10 kHz and ~ 21 W for 20 kHz.

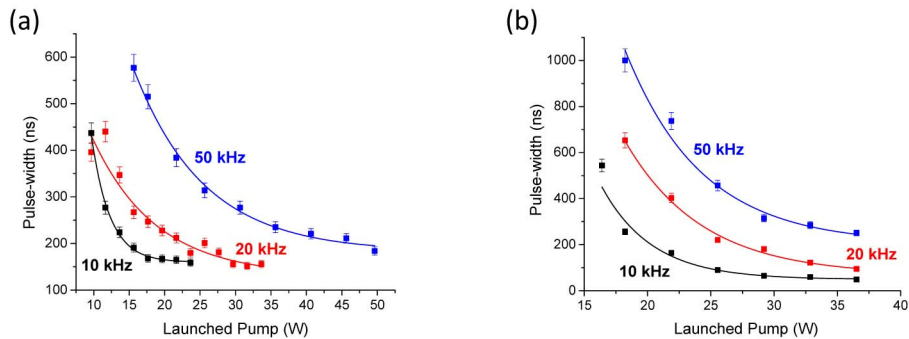


Fig. 6. Evolution of pulse duration with absorbed pump for a) LMA and b) PCF at different repetition rates.

In order to determine if the severe degradation in usable power is the result of ASE, we first measured the P_{use} polarization extinction ratio (PER) and found to be above 20 dB. Second, we inserted an electro-optic pulse picker at the output of the step-index fiber oscillator which functioned as a temporal gate with 125 ns gated duration. $\sim 94\%$ of power was measured to be within the gate, with the 6% loss due to transmission through the waveplate, polarizer, and Pockels cell of the pulse picker. 10 kHz repetition rate was chosen, as it was the lowest repetition rate that provided stable output pulses. Repetition rates lower than 10 kHz generate pulses with higher amplitude jitter as the pulse extraction rate approaches the 650 μs upper state lifetime (3F_4 to 3H_6 transition) in thulium-doped silica [22]. The PCF oscillator was not tested for ASE, as it did not exhibit a similar degradation in performance.

5. Discussion

Despite similar P_{total} output powers at 10 kHz, the maximum usable pulse energy is only 273 J for the step-index fiber laser system as compared to 435 J for the PCF laser. Even more striking, the maximum usable peak power is 8.9 kW in the PCF vs. only 1.8 kW for the step-index fiber in a Q-switched oscillator. Our analysis demonstrates that there is a significant difference in Q-switched oscillator performance as a result of power being lost to cladding light in the step-index fiber.

Given that the degradation in usable output is independent of laser repetition rate, thermal modification of the fiber waveguide does not explain this behavior. Furthermore, the correlation between the drop in the percentage of usable power and the minimum pulse duration in the step-index fiber leads us to believe that the gain for the fundamental mode saturates to such a level that gain for HOM generation becomes comparable. Based upon the S^2 data, it is clear that the step-index fiber supports significantly more light in HOMs than the PCF. Since these HOMs experience significantly higher propagation loss, the majority of light generated in and/or coupled into them will be lost to the cladding. This explanation provides the best agreement with experimental observation and illustrates an important advantage of the PCF for use in high-energy Q-switched oscillators.

On the other hand, the PCF also has several notable disadvantages relative to the step-index fiber. Since it was not spliced to passive fiber, the entire active fiber could not be cooled and hence the maximum pump light launched into the PCF was limited to ~ 40 W to minimize the possibility that heating could soften/melt the polymer coating near the fiber end facet leading to misalignment of the pump and destruction of the fiber facet. In addition, the step-index fiber laser has a lower laser threshold and can achieve slightly higher slope efficiencies than the PCF based laser. Importantly, so far we have not observed 2-for-1 photon excitation through cross-relaxation in the Tm:PCF. Finally, packaging and integration of PCF is significantly more difficult due to the relatively large bend diameter, >35 cm, required to avoid excessive bend losses for the fundamental mode and the higher difficulty of fabricating all-fiber pump combiners for PCF [23] when compared to conventional components based on step-index fiber.

Comparing our oscillator results with experiments in an amplifier configuration, it has to be noted that in the latter case the HOMs have less significance. As an amplifier medium, Tm-doped step-index LMA fiber has proven reliable, effective performance [5,6,24] and quasi-single mode, multi-mJ ns pulsed operation [25]. We have demonstrated >100 W cw amplification in LMA with $M^2 < 1.25$ and $<10\%$ of signal light in the cladding [26], and believe that HOMs are less likely to be excited in such amplifier configurations (assuming optimized launching conditions) than in an oscillator configuration.

6. Conclusion

Combining S^2 imaging with studies of the performance of 2 μm large mode fibers in Q-switched fiber laser oscillators reveals the impact of HOMs on the laser performance. In the case of the LMA step-index fiber, the usable power decreases from 80% to $<60\%$ as usable pulse energy reaches 250 μJ while no such degradation is observed when using quasi single-mode PCF to generate pulse energy >400 μJ . This degradation appears to occur due to saturation of the gain for the fundamental mode leading to a greater percentage of power in HOMs, which in turn is lost through coupling into the cladding. We believe PCFs are more resistant to this degradation due to the significantly lower percentage of power guided in HOMs.

Acknowledgments

The authors acknowledge the support of the Joint Technology Office through the High-Energy Laser Multidisciplinary Research Initiative (grant numbers W911NF0510517 and W911NF1010441), the European Commission IMPROV project (grant number 257894) and the State of Florida.